



# Optical nonlinearity, limiting and switching characteristics of novel ruthenium metal-organic complex



K.B. Manjunatha<sup>a,\*</sup>, Ravindra Rajarao<sup>b</sup>, G. Umesh<sup>c</sup>, B. Ramachandra Bhat<sup>d</sup>, P. Poornesh<sup>e</sup>

<sup>a</sup> Department of Physics, NMAM Institute of Technology, Nitte 574110, India

<sup>b</sup> Centre for Sustainable Materials Research and Technology, School of Materials Science and Engineering, University of New South Wales, Sydney, NSW 2052, Australia

<sup>c</sup> Optoelectronics Laboratory, Department of Physics, National Institute of Technology Karnataka, Mangalore 575025, India

<sup>d</sup> Catalysis and Materials Laboratory, Department of Chemistry, National Institute of Technology Karnataka, Mangalore 575025, India

<sup>e</sup> Nonlinear Optics Research Laboratory, Department of Physics, Manipal Institute of Technology, Manipal University, Manipal 576 104, Karnataka, India

## ARTICLE INFO

### Article history:

Received 16 March 2017

Received in revised form

24 May 2017

Accepted 27 June 2017

Available online 1 July 2017

### Keywords:

Nonlinear optics

Z-scan

DFWM

Optical limiting

## ABSTRACT

We report the nonlinear optical properties of Ruthenium metal complex a promising organic material for use in scientific and technological applications. The thin films of newly synthesized ruthenium metal–organic complex were fabricated using spin coating technique. Z-scan and degenerate four wave mixing (DFWM) techniques used to extract the third-order nonlinear optical (NLO) parameters. The data reveals the investigated material exhibited relatively large NLO properties. The pump–probe experiments shows that the switch-on and off times of the material were in the order of  $\mu\text{s}$  at different pump intensities and the energy dependent transmission studies reveal good limiting property of the material in nanosecond regime.

© 2017 Elsevier B.V. All rights reserved.

## 1. Introduction

Metal-organic or organometallic materials have received significant interest over the past decade because of their large NLO properties and have possible applications in optical devices such as all-optical switching, power limiters etc [1–4]. High nonlinearity, ease in structural modifications, relatively cheap and ease in synthesis make these materials more attractive and have the capability of replacing the inorganic systems [5]. Organometallic systems obtained by the incorporation of transition metal ions into organic systems, which introduces more sublevels into the energy hierarchy, thus permitting more allowed electronic transitions and resulting in larger NLO effects. The advantages of organometallic systems are by changing metal ion and/or surrounding organic environment we can tune the NLO properties [5–7].

Keeping this in mind, we synthesized new salophene based ruthenium complex and investigated the NLO properties using Z-scan and DFWM technique. To explore the suitability of the

material for photonic device applications, all-optical switching and optical power limiting measurements were carried out using pump-probe and energy dependent transmission techniques respectively.

## 2. Experimental techniques

### 2.1. Materials and methods

Analytical grade chemicals were used. Solvents were purified and dried according to standard procedure (Vogel 1989). Ruthenium (III) chloride trihydrate and all other reagents were procured from Sigma Aldrich Chemicals, and were used without further purification. The synthesis of ligand, salophene (L) = *N,N'*-disalicylidene-1,2-ethylenediamine dianion is reported in elsewhere [8].

The Ru(II) Schiff base complex, Ru (salophene) (H<sub>2</sub>O) (Cl) (named as Ru-L) was prepared in high yield via the interaction of the free Schiff base, H<sub>2</sub>L, with RuCl<sub>3</sub>·3H<sub>2</sub>O in a 1:1 mol ratio in refluxing absolute ethanol for 12 h. Ru-L: <sup>1</sup>H NMR (DMSO-*d*<sub>6</sub>):  $\delta$  8.40 (s, 2H, HC=N), 7.88–7.86 (m, 2H, ArH), 7.37–7.34 (m, 2H, ArH), 7.03 (d, J 7.6 Hz, 2H, ArH), 6.86 (d, J 7.6 Hz, 2H, ArH) and 6.44 (t, J 7.6 Hz, 2H, ArH). IR (cm<sup>-1</sup>, KBr): 3314 m, 1613 s, 1585 s, 1540 s,

\* Corresponding author.

E-mail addresses: [manjukb15@nitte.edu.in](mailto:manjukb15@nitte.edu.in) (K.B. Manjunatha), [poorneshp@gmail.com](mailto:poorneshp@gmail.com) (P. Poornesh).

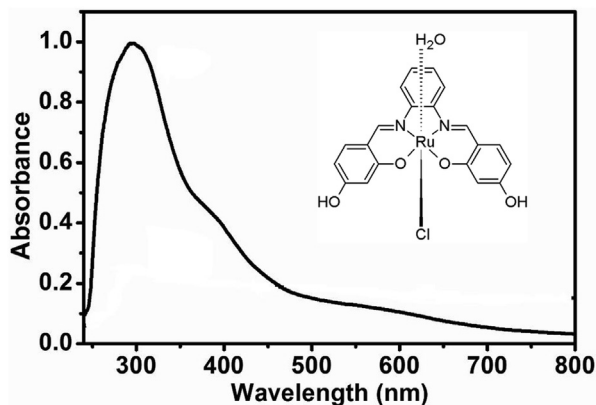


Fig. 1. UV–visible absorption spectrum of the sample Ru-L. Inset Molecular Structure of Ru-L.

1467 s, 1444 s, 1389 m, 1238 s, 1193 s, 1107 m, 975 m, 737 s.

NLO properties were investigated in both liquid and solid form. Liquid samples of different concentrations were obtained by dissolving material into *N,N*-dimethylformamide (DMF). Solid samples of different concentrations were fabricated using spin coating technique [9]. The Z-scan and DFWM techniques were used to determine the NLO properties of the samples [10–16]. Optical power limiting studies of the samples carried out by energy dependent transmission technique [9]. All-optical switching characteristics were performed using standard pump-probe technique [9,16].

### 3. Results and discussion

The molecular structure and UV–Vis absorption spectra of the sample are shown in Fig. 1. The peaks between 230 and 350 nm are attributed to intra-ligand charge transfer transitions and small peak in between 390 and 500 nm represents the DMSO-*d*<sub>6</sub> forbidden transitions.

#### 3.1. Z-scan studies

The open aperture Z-scan technique was used to obtain the magnitude and sign of nonlinear absorption (NLA) coefficient ( $\beta_{eff}$ ) of the sample. Fig. 2 shows the open aperture Z-scan curves of the sample with theoretical fits [10,17] and characteristics of the curve suggests the intensity dependent absorption of the sample. Reverse saturable absorption (RSA) via excited state absorption (ESA) is attributed for large NLA in the sample, this can be explained with

five-level model reported in the literature [17]. The excited state absorption cross section  $\sigma_{exc}$ , can be measured using the normalized energy transmission of open aperture Z-scan [18–21].

$$T = \ln \left( 1 + \frac{q_0}{1 + x^2} \right) / \left( \frac{q_0}{1 + x^2} \right), \quad (1)$$

where  $q_0 = \frac{\sigma_{exc} \alpha F_0(r=0) L_{eff}}{2h\nu}$ ,

$X = z/z_0$ ,  $z$  is the distance of the sample from the focus,  $z_0$  is the Rayleigh length given by the formula  $Z_0 = k\omega_0^2/2$ , where  $k$  is the wave vector and  $\omega_0$  is the beam waist at the focus  $L_{eff} = [1 - \exp(-\alpha L)]/\alpha$ , and  $F_0$  is the on-axis fluence at the focus.

The value of excited state absorption cross section  $\sigma_{exc}$ , were obtained by fitting the open aperture data using equation (1) and the ground state absorption cross section,  $\sigma_g$ , were calculated using the relation given below and the values are given in Table 1,

$$\alpha = \sigma_g N_a C, \quad (2)$$

where  $N_a$  is the Avogadro's number and  $C$  is the concentration in mol/L.

The magnitude of ESA cross-section,  $\sigma_{exc}$  larger than ground-state absorption cross-section,  $\sigma_g$  of the sample suggests that the NLA is due to RSA. In Fig. 3, the value of  $\beta_{eff}$  decreases while increasing the on-axis intensity  $I_0$  which is evident of NLA due to RSA [22]. The closed aperture Z-scan technique was used to obtain the pure nonlinear refraction. Fig. 4 shows the pure nonlinear refraction Z-scan curves with theoretical fits of the sample. The signature of the curve indicates the nonlinear refractive index ( $n_2$ ) is negative (self-defocusing effect). The magnitude of  $n_2$  and  $\text{Re}\chi^{(3)}$  were determined and tabulated in Table 1. The thermal effects were taken in to account in the experiments by performing in the single shot mode. More over the closed aperture z-scan curve displays a peak-valley separation of less than  $\sim 1.7Z_R$ . A peak-valley separation of more than 1.7 times the Rayleigh range ( $Z_R$ ) is the signature of thermally induced nonlinearity and hence thermal effects can be neglected. Hence, the observed nonlinearity is predominantly electronic in nature, in addition there is a possible presence of orientational contribution to the observed nonlinearity [23].

#### 3.2. DFWM studies

The magnitude of  $\chi^{(3)}$  was also determined using DFWM technique. The variation of DFWM signal with pump energy of CS<sub>2</sub> and sample are shown in Fig. 5 where the solid line is the cubic fit to the experimental data. The  $\chi^{(3)}$  data of the sample was obtained by comparing the DFWM signal of CS<sub>2</sub> and calculated using the following equation [24],

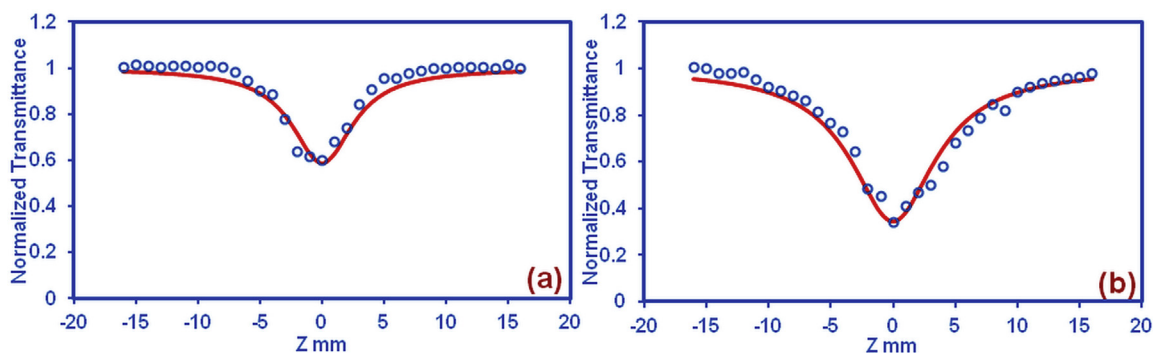


Fig. 2. Open aperture Z-scan of (a) sample in liquid form at the concentration of  $2.5 \times 10^{-4}$  mol/L and (b) sample in solid form at the concentration of 0.5 wt%. In (a) and (b) solid line depicts theoretical fit.

Download English Version:

<https://daneshyari.com/en/article/5442504>

Download Persian Version:

<https://daneshyari.com/article/5442504>

[Daneshyari.com](https://daneshyari.com)